Predicting post-mortem meat quality in porcine *longissimus lumborum* using Raman, Near Infrared and Fluorescence spectroscopy

Petter Vejle Andersen [a]*, Jens Petter Wold [a], Eli Gjerlaug-Enger[b], Eva Veiseth-Kent [a]

[a] Nofima, Osloveien 1, 1430 Ås, Norway

[b] Norsvin, Storhamargata 44, 2317 Hamar, Norway

E-mail adresses:

Petter Vejle Andersen: petter.andersen@nofima.no

Jens Petter Wold: jens.petter.wold@nofima.no

Eli Gjerlaug-Enger: eli.gjerlaug@norsvin.no

Eva Veiseth-Kent: eva.veiseth-kent@nofima.no

*Corresponding author at: Nofima, Osloveien 1, 1430 Ås, Norway. Tel.: +47 64 97 04 90.

ABSTRACT

Spectroscopic techniques can provide valuable information about post-mortem meat quality. In the current study, Raman, NIR and fluorescence spectroscopy was used to analyze pH, drip loss and intramuscular fat in pork *longissimus lumborum* (n = 122) at 4-5 days post-mortem. Results were promising for partial least squares regression (PLSR) from Raman spectroscopy, giving coefficients of determination from cross validation (r_{cv}^2) ranging from 0.49 to 0.73 for all attributes examined. Important regions in the PLSR models from Raman spectroscopy were attributed to changes in concentrations of post-mortem metabolites and modifications of protein secondary structure. Near infrared and fluorescence spectroscopy showed limited ability to analyze quality, with r_{cv}^2 ranging from 0.06 to 0.57 and 0.04 to 0.18, respectively. This study encourages further research on the subject of Raman spectroscopy as a technique for meat quality analysis.

Keywords

Water-holding capacity; pH; intra muscular fat; Raman spectroscopy; NIR spectroscopy; fluorescence spectroscopy

1. INTRODUCTION

One of the most important quality parameters for pork is water-holding capacity (WHC), affecting monetary value, processing properties (Torley, D'Arcy, & Trout, 2000) and eating quality (Hughes, Oiseth, Purslow, & Warner, 2014). Many factors influence WHC of meat, including rate of post-mortem pH decline and ultimate pH (pH_u) (Warriss & Brown, 1987), proteolysis (Huff-Lonergan & Lonergan, 2005) and chemical composition of meat (e.g. intramuscular fat (IMF)) (Lawrie, 1985), illustrating the complexity of this property. WHC of fresh meat is usually measured as amount of drip formed from an intact meat sample, e.g. the bag method (Honikel, 1998) and EZ-DripLoss method (Rasmussen & Andersson, 1996), which are invasive, labor- and time-consuming methods. Even the standard method for measuring pH requires a glass probe to be inserted into the meat and manually recording the pH-value. Development of rapid and non-invasive methods for meat quality assessment for on-line or at-line application is consequently of interest to the meat industry, for amongst others meat classification and optimization of production procedures. To this end, there have been many studies conducted utilizing spectroscopic techniques to analyze pH, WHC and chemical composition of meat. The most promising techniques for implementation in the abattoir are near infrared (NIR), Raman and fluorescence spectroscopy, because they are all non-invasive and rapid techniques that can be implemented in an abattoir.

NIR spectroscopy has great potential for meat quality analysis because the technique measures absorption corresponding to overtones and combinations of vibrational modes involving C–H, O–H and N–H chemical bonds, which in principle makes it possible to analyze composition and functional properties of meat (Osborne, 2006). The use of NIR spectroscopy for meat analysis has been thoroughly reviewed within the last decade, showing the substantial effort put forth in this field (Prieto, Pawluczyk, Dugan, & Aalhus, 2017; Prieto, Roehe, Lavin, Batten, & Andres, 2009; Weeranantanaphan, Downey, Allen, & Sun, 2011). To the best of our knowledge, the benchmark of performance for VIS-NIR spectroscopy performed on pork are as follows: pH: coefficient of determination (r_{cv}^2) = 0.82 and root mean square error of cross validation (RMSECV) = 0.10 (Liao, Fan, & Cheng, 2010); drip loss: r_p^2 = 0.76 and root mean square error of prediction (RMSEP) = 0.8% (Kapper, Klont, Verdonk, Williams, & Urlings, 2012); and IMF: r_{cv}^2 = 0.96 and RMSECV = 0.46% (Prevolnik et al., 2005). Although many studies have shown great promise, no NIR instruments for commercial use for prediction of pH and WHC have been developed.

Raman spectroscopy can provide information about proteins, such as peptide backbone structure and amino acid side-chain properties, as well as characterization of fat, making it a suitable technique for analysis of meat quality (Li-Chan, 1996). Raman spectroscopy was first used for analysis of WHC in pork in 2003 and the results were very promising (r_{cv}^2 = 0.98 and RMSECV = 0.27), but the sample size was small (n = 14) and the authors cited a need for further attention in future studies (Pedersen, Morel, Andersen, & Balling Engelsen, 2003). Raman spectroscopy has gained some traction for pork quality analysis in the last few years with the development of a handheld Raman instrument (Schmidt, Sowoidnich, & Kronfeldt, 2010). Results of pH_u and drip loss predictions have been promising from Raman spectra acquired between 30 and 120 min post-mortem in the abattoir, being able to predict pH_u with r_{cv}^2 = 0.68 and RMSECV = 0.09 and drip loss with r_{cv}^2 = 0.73 and RMSECV = 1.0% in one study (Scheier, Bauer, & Schmidt, 2014), and pH with r_{cv}^2 = 0.31 and RMSECV = 0.05 and drip loss with r_{cv}^2 = 0.52 and RMSECV = 0.6% in a follow-up study (Scheier, Scheeder, & Schmidt, 2015). We are unaware of any studies using Raman spectroscopy to analyze IMF of intact pork, but a study has been conducted for lamb meat, resulting in a r_{cv}^2 = 0.02 and RMSECV = 1.2% for IMF (Fowler, Ponnampalam, Schmidt, Wynn, & Hopkins, 2015).

Not many studies have been conducted using fluorescence spectroscopy to analyze fresh pork quality. One of the few studies analyzing fresh pork quality with fluorescence was carried out by Brondum et al. (2000), where drip loss was predicted with r^2 = 0.68 and SEP = 2.27% and IMF was predicted with r^2 = 0.57 and SEP = 1.09%. Fluorescence spectroscopy has also shown promise to analyze pH in a model system containing isolated myofibrils from pork (Andersen, Veiseth-Kent, & Wold, 2017), encouraging further research in this area.

The main aim of this work was to investigate the potential for Raman, NIR and fluorescence spectroscopy to predict drip loss and measure pH_u of fresh pork, with a secondary aim to measure IMF. Using three spectroscopic techniques on the same set of samples allows for comparison of spectroscopic techniques under similar conditions, possibly indicating which techniques should be the focus in future research.

2. MATERIALS AND METHODS

2.1 Animals and meat quality analyses

A selection of 122 Norwegian Landrace boars from an ongoing testing program at Norsvin's boar test station in southeastern Norway were part of this study. The boars were fed ad libitum on conventional concentrates, and the average start and end weight at the test station was 35

to 120 kg live weight, respectively. The boars were slaughtered in eight batches at a commercial abattoir over a period of 9 months. The animals were stunned with 90% CO_2, followed by exsanguination, scalding and splitting within 30 min post-mortem. After 45 min the carcasses were transported through a cooling tunnel (-22 °C, air velocity 8-10 m/s). Following this, the carcasses were chilled in a cooler at 1 °C to 3 °C for 20 h until a core temperature of 7 °C was reached. Finally, the carcasses were transported to a partial dissection line at Animalia, the Norwegian Meat and Poultry Research Centre.

At 4 or 5 days postmortem, the loin muscle (LL – *Longissimus lumborum*) was dissected from the right side of the carcasses, trimmed for fat and used for assessment of multiple meat quality traits and spectroscopic measurements as described in the following. Ultimate pH was measured at the last rib curvature using an insertion pH electrode (WTW 82362, pH 330i, Welheim, Germany). A 5-cm slice of the muscle (positioned 2 cm anterior and 3 cm posterior to the last rib curvature) was homogenized by grinding for 30 s using a mixer (Robot Coupe r5a+, W 1100, Robot Coupe, USA, Inc.) for subsequent measurement of IMF as described by Gjerlaug-Enger, Aass, Odegard, and Vangen (2010).

Assessments of drip loss were performed using two different methods, the EZ-DripLoss method and purge loss in vacuum packages. For the EZ-DripLoss measurement (Rasmussen & Andersson, 1996), two samples at fixed locations on a 2-cm slice (positioned 3 to 5 cm posterior to the last rib curvature) were cut using a circular knife (2.5 cm diameter). Samples were placed in drip loss containers (C. Christensen ApS, Denmark), and stored at 4 °C for 24 h, after which the weight of the drip loss was measured, and expressed as a percentage of the initial sample weight. For the purge loss measurement, a 5-cm thick slice (positioned 8 to 13 cm posterior to the last rib curvature) was weighed before being placed in a plastic bag and vacuum packed using 98% vacuum. The vacuum packed slices were placed in a single layer on a rack in a cooler (4 °C), and stored for 8 days, after which the bags were opened, and the meat gently dabbed with paper before weighing again. Purge was calculated as a percentage of the initial sample weight.

2.2 Spectroscopic analysis

A freshly cut slice of approx. 3 cm (positioned 5 to 8 cm posterior to the last rib curvature) from *LL* was used for spectroscopic analyses at 4-5 days post-mortem. All samples were analyzed with NIR spectroscopy first, followed by fluorescence spectroscopy and finally Raman spectroscopy.

2.2.1 NIR spectroscopy

The meat slice designated for spectroscopy was cut and mounted in a Rapid content module sample cell (FOSS Analytical, Hillerød, Denmark). A spectrum from a sample surface with a diameter of 17.25 mm was recorded at eight different locations on the meat surface using an XDS Rapid content analyzer (FOSS Analytical, Hillerød, Denmark) measuring in the 400-2500 nm wavelength region at 0.5 nm intervals. Spectra were recorded as log(1/R) with FOSS NIRSystem Vision software. All spectra from one sample were averaged prior to further analysis.

2.2.2 Fluorescence spectroscopy

Fluorescence was measured in front face mode on the same sample surface as was measured with NIR. The measurements were carried out with a FluoroMax-4 (Horiba Scientific, Edison, NJ, USA) in front face mode via a FL-300/FM43000 bifurcated fiber-optic probe (Horiba Scientific). The distance between the probe head and sample was about 5 cm and created a circular measurement area of 40 mm diameter. Probe and sample were covered by a black shield to avoid ambient straylight. Emission spectra in the region from 300 to 500 nm (2 nm intervals) were recorded for excitation at 292 nm.

2.2.3 Raman spectroscopy

The sample was cut into three slices and one spectrum was recorded from the freshly cut surface of each slice using a Kaiser RamanRXN2™ Multi-channel Raman analyzer (Kaiser Optical Systems, Inc., Ann Arbor, MI, USA) with a spectral resolution of 5 cm^{-1}. The spectrometer was equipped with a 785 nm laser and PhAT probe, measuring a spot size of 6 mm in diameter. The spectra were recorded with a laser power set to 400 mW in the range of 150-1890 cm^{-1} with 0.3 cm^{-1} intervals and exposure of 3 times 15 s was used for acquisition. Instrument set-up and experiment was controlled using iC Raman version X software (Mettler Toledo, Greifensee, Switzerland).

2.3 Pre-processing of spectra and data analysis

2.3.1 Pre-processing of spectra

Pre-processing of spectral data was done to give comparable spectra for further analysis, by reducing or removing the impact of noise, scatter effects and other undesirable alterations in the spectra.

The three Raman spectra from each sample were averaged. The oxygen peak from 1530 to 1570 cm^{-1} was removed from the spectra by cutting out the variables from the spectrum

matrix prior to further pre-processing in the range from 450 to 1775 cm^{-1}. Raman spectra were first base-line corrected and fluorescence background was removed using polynomial curve-fitting (Lieber & Mahadevan-Jansen, 2003), before second order extended multiplicative scattering correction was applied (EMSC) (Liland, Kohler, & Afseth, 2016). The NIR spectra were divided into two regions, 400 to 1850 nm and 780 to 1850 nm, before standard normal variate (SNV) algorithm (Barnes, Dhanoa, & Lister, 1989) was applied to each region separately. Fluorescence spectra were pre-processed by SNV.

2.3.2 Data analysis

Partial least squares regression (PLSR) was used for determining relationships between reference measurements and spectroscopic data. PLSR emphasizes information in the spectra that is important for explaining variation in the reference measurements when making models (Martens & Martens, 2001). PLSR models were cross-validated by randomly dividing all samples in four segments, leaving one segment out at a time for validation, and using the same segments for all spectroscopic methods. An uncertainty test was performed for the PLSR models to give information about important variables in the models (Martens & Martens, 2000), and to use these variables to investigate if more reliable models could be made by using only the important variables. The principle for the uncertainty test is to analyze the stability of the β-coefficients from the sub-models developed during cross-validation, and the significantly stable variables are marked in the final model. Ratio of prediction to deviation (RPD) values were calculated as the standard deviation of the reference values divided by the models RMSECV to give a quick appraisal of a model (Williams & Sobering, 1993). The following guidelines are given for evaluating RPD values and the recommended application of the model when analyzing biological samples: RPD < 2: very poor, not recommended; 2.0 < RPD < 2.4: poor, rough screening; 2.5 < RPD < 2.9: fair, screening; 3.0<RPD<3.4: good, quality control; 3.5<RPD<3.9: very good, process control, and 4.0<x: excellent, any application (Williams, 2014).

PLSR was performed in the following spectral regions: Raman: 450 to 1800 cm^{-1}; NIR: for pH: 400 to 1850 nm, for drip loss and IMF: 780 to 1850 nm; fluorescence: emission from 306 to 412 nm.

Pre-processing of Raman spectra were carried out using Open EMSC toolbox for MATLAB freely downloadable from http://nofimaspectroscopy.org in MATLAB version R2013b (The MathWorks, Natick, MA), while pre-processing of NIR and fluorescence spectra were carried

out in The Unscrambler® X version 10.4 (CAMO Process AS, Norway). PLSR models were developed using The Unscrambler® X version 10.4 (CAMO Process AS, Norway).

3. RESULTS AND DISCUSSION

3.1 Reference meat quality measurements

Results from reference analyses are summarized in table 1 and correlations between reference measurements are shown in table 2. The distribution of the reference measurements seemed to be sufficient for modelling purposes, since the standard deviation divided by range was 0.21 for all analyses. The range of pH_u and drip loss measurements were considered as reflective of what is expected in Norwegian landrace pigs, while the IMF content was relatively low in the current study. The reference measurements were conducted later than what is typical for studies regarding pork quality, 4-5 days post-mortem, as opposed to the more common 24 h (Christensen, 2003; Otto, Roehe, Looft, Thoelking, & Kalm, 2004). This could have affected some of the reference measurements, for instance, drip loss can be influenced by post-mortem proteolysis (Gardner, Huff Lonergan, & Lonergan, 2005). The reason for conducting analyses at 4-5 days post-mortem was that this is a procedure established by the collaborating pig-breeding association. They analyze thousands of pigs yearly, which have led to highly standardized operating procedures for meat quality analysis.

Of note when comparing the two drip loss measurements is that the EZ-DripLoss measurement had a larger range than the vacuum drip (VD), even though the measurement for EZ-DripLoss was conducted over a 24 h period, as opposed to 8 d for VD. This is likely caused by the more invasive procedure and larger surface area to volume of the EZ-DripLoss method and that the VD samples might have an upper limit of drip formation attributed to physical constraints of the vacuum bag. Another cause for lower drip loss in vacuum packed samples could be reabsorption of water during storage, as hypothesized by Kristensen and Purslow (2001). The correlation between the two measurements was 0.60, meaning that they most likely measure different phenomena related to drip formation, e.g. the impact of vacuum packing or the effect of sample morphology.

The correlation of pH_u and IMF with the drip measurements showed the same tendency for both drip methods, where low values for pH and IMF were significantly correlated with high drip. This correlation was stronger for EZ-DripLoss than for VD, even though their SD/range values were comparable. This implies that the EZ-DripLoss measurement could be closer related to physical attributes of the meat than the VD measurement, thus giving reason to

believe that EZ-DripLoss measured more of the inherent meat characteristics while VD to a larger extent was influenced by the method. However, it is still of interest to investigate if VD can be predicted by spectroscopic techniques, as this is how meat is often presented to consumers. Additionally, there is no golden standard for measurement of drip loss in meat, meaning that the method of measuring drip loss needs to be tailored to the specific applications.

3.2 Spectroscopy

A summary of the performance for PLSR models from NIR, fluorescence and Raman spectroscopy and reference measurements is shown in table 3. It was evident that models from Raman spectroscopy performed better than NIR and fluorescence for all reference measurements, and that NIR performed better than fluorescence. The RPD for each model ranged from 1.01 to 1.93, meaning that no model meets the recommended threshold for rough screening at 2.0 (Williams, 2014). Nevertheless, the models based on Raman spectroscopy seemed to be suitable for rough sorting of samples in batches according to their predicted values (Fig. 1). For instance, by selecting 20% of the samples with highest predicted EZ-DripLoss from the PLSR model and comparing the reference measurement of EZ-DripLoss from these samples with the remaining 80% of samples, there was an average of 2.2% ($p<0.001$) higher EZ-DripLoss in the high predicted drip loss group. Batches of meat with higher drip loss can be sorted from the rest and used in products where the inferior quality is accounted for, such as canned pork (Florowski et al., 2017), while simultaneously increasing the average quality of the remaining pork.

Model performance has to be considered in relation to the error of the reference analysis, which is difficult to obtain for drip loss measurements because it is impossible to analyze the same sample twice. It is possible to estimate this error by measuring adjacent samples, but then it is important to acknowledge that there is an inherent difference in drip loss, both longitudinal and transversal, along the entire *longissimus thoracis et lumborum* (Christensen, 2003; Otto et al., 2004).

When performing PLSR it was discovered that some samples could be considered as outliers. For EZ-DripLoss, one sample was poorly described by all spectroscopic methods, giving strong reason to believe that something went wrong when conducting the reference measurement. This happened for one of the sample batches for VD; therefore, the entire batch (19 samples) was left out when conducting both PLSR and correlation analyses between reference measurements. Manual inspection of NIR spectra revealed two severely deviating

spectra, and these were consequently left out of all NIR PLSR models. It is also worth noting that the model performance improved a lot by removing a few samples with high residual sample calibration variance for reference measurements (Y-variance) for most models, without changing the important variables in models, suggesting that some of the reference measurements or spectra might have been incompatible or that the reference measurements could be considered as outliers. For instance, by removing 12 samples (n = 110) in the model from Raman spectroscopy and EZ-DripLoss, the model improved to give a r_{cv}^2 = 0.76 and a RMSECV of 0.83, resulting in an RPD > 2.0, which is sufficient for rough screening.

3.2.1 Raman spectroscopy

It is useful to identify which spectral regions are important for establishing the relationship between spectroscopy and reference measurements for elucidating the qualitative association to known changes in post-mortem meat. To evaluate which spectroscopic regions are important for the models, the weighted regression coefficients for the best models for each reference analysis were evaluated (Fig. 2). The changes in Raman spectra related to reference measurements of pH_u and drip loss could in general be categorized in two groups, one being related to post-mortem metabolism and the other being changes in protein secondary structure.

For pH_u, the important regions related to metabolism from the PLSR model were at 973 cm^{-1} and 1045 cm^{-1}, which have been assigned to the PO_3^{2-} stretching vibration of the phosphate moiety (Rimai, Cole, Parsons, Hickmott, & Carew, 1969) and creatine (Cr) or lactate in meat (Scheier, Kohler, & Schmidt, 2014), respectively. The phosphate signal at approx. 980 cm^{-1} is stronger under more basic conditions (Scheier & Schmidt, 2013), likely contributing to the positive correlation in the model. Conversely, peaks attributed to phosphate at approx. 880 cm^{-1} and 1080 cm^{-1} are expected to increase as pH decreases (Scheier & Schmidt, 2013), but this was only detected for the peak at 880 cm^{-1} in the current study. The reason for not detecting a change at 1080 cm^{-1} might be that this region contains signals from other Raman active molecules, such as glycogen and adipose tissue, thus obscuring the relatively low signal from phosphates. As concentration of lactate increases post-mortem, pH decreases, thus giving a negative correlation for the peak at 1045 cm^{-1}. For the EZ-DripLoss and VD models, the region at 977 cm^{-1} had an opposite sign compared to the pH model, most likely caused by the inverse relationship between pH and drip loss. The EZ-DripLoss model introduced contributions from another molecule related to metabolism in the region at approx. 880 cm^{-1}, attributed to the acidic form of inorganic phosphate (Scheier, Kohler, et al., 2014).

Important regions related to protein secondary structure changes were in the amide I and amide III regions, where the bands at 1635 cm^{-1}, 1269 cm^{-1} and 942 cm^{-1} are assigned to α-helical structures and the bands at 1685 cm^{-1} and 1237 cm^{-1} are assigned to β-sheet structures (Krimm & Bandekar, 1986; Tu, 1986). Intensity of regions related to α-helical structures increased with increased pH, while intensity of regions related to β-sheet structures decreased with increased pH. As noted for metabolites, the relationship in the models is opposite for drip loss models compared to models from pH. These changes might be caused by increased denaturation of proteins when pH declines rapidly post-mortem (Joo, Kauffman, Kim, & Park, 1999), and similar changes to protein secondary structure have been shown to be a direct consequence of changes in pH (Andersen et al., 2017).

The important regions for the IMF model were all in close proximity to some of the characteristic peaks from pork adipose tissue, most prominent at 802 cm^{-1}, 1296 cm^{-1}, 1438 cm^{-1} and 1655 cm^{-1} (Beattie, Bell, Borgaard, Fearon, & Moss, 2006), but some of the regions were also close to protein secondary structure regions (e.g. amide I). As IMF content was relatively low in the analyzed samples, and the characteristic fat peaks (at e.g. 1296 cm^{-1} and 1438 cm^{-1}) were only clearly visible in a few of the samples, it is plausible that the model relies on collinear regions from other molecular structures or the high correlation between fat and protein concentration in meat (Isaksson, Nilsen, Togersen, Hammond, & Hildrum, 1996). For improving the model for IMF predictions, effort should be put forth to make models where larger variation in IMF is included.

The overlap of vibrations from fat and proteins highlights one of the difficulties when developing models for meat quality assessments, namely that it is difficult to distinguish the influence of one meat component from another. One of the traditionally limiting factors for Raman spectroscopy is the small sample area analyzed, which was improved in the current study by using a probe with a laser spot diameter of 6 mm. Conversely, the increased spot size comes at the cost of including strong scattering from IMF. Future studies are needed to investigate the impact of scattering from fat on the validity of models for other quality parameters from Raman spectroscopy concerning meat quality, as spectra with a fat signature purposely have been avoided by others (Scheier, Bauer, et al., 2014; Scheier et al., 2015).

PLSR models developed in the current study performed on a comparable level to those developed by Scheier, Bauer, et al. (2014) and Scheier et al. (2015) for pH and drip loss predictions. Our results emphasized many of the same spectral regions as the two cited studies, thus strengthening the evidence for the importance of regions related to metabolites

and protein secondary structure for predicting pH and drip loss. One important difference in the current study compared with the work of Scheier et al. (2014; 2015) is the time of measurement, where theirs were done on pre-rigor muscle at 30-120 min post-mortem, the analysis in the current study was performed on post-rigor muscle at 4-5 days post-mortem, making it harder to directly compare the results. Regarding estimation of IMF, results from the current study showed vastly improved model performance compared to a study on lamb (Fowler et al., 2015). This is most likely caused by the larger laser diameter in the current study, thus measuring a larger sample area (approx. 14000 times increase in measuring area).

3.2.2 NIR spectroscopy

Inspection of important regions of models from NIR spectroscopy was only meaningful for pH and IMF models, as the regression coefficients for drip loss did not reveal large enough stable regions and were rather noisy. The most important regions for the pH model were mainly in the visible part of the spectra, from 400 nm to 780 nm, likely caused by the correlation between color and pH (Joo et al., 1999), in addition to a stretch at 1410 nm to 1435 nm and a stretch from 1750 nm to 1850 nm. The stretch from 1410 nm to 1435 nm is attributed to water and it may be related to the strength of hydrogen bonds or the amount of water in the analyzed area (Segtnan, Sasic, Isaksson, & Ozaki, 2001). The longer stretch from 1750 nm to 1850 nm can be attributed to a mix of CH and OH vibrations (Li-Chan, Ismail, Sedman, & van de Voort, 2002). For the IMF model two regions were important, one from 1690 nm to 1708 nm, and a second from 1720 nm to 1735 nm, assigned to protein and fat, respectively (Williams & Norris, 2001). The model β-coefficients were positive for fat and negative for protein, again emphasizing the inverse correlation between these parameters. This shows that some regions seem to have chemical information relevant for interpretation (e.g. 1720 nm to 1735 nm for IMF), while some important regions seem to rely on non-chemical information which is difficult to interpret (e.g. 1750 nm to 1850 nm for pH).

The NIR models did not perform well compared to previous studies on fresh pork (Kapper et al., 2012; Liao et al., 2010; Prevolnik et al., 2005). A number of factors may have caused this discrepancy in the current study compared with others, including number of samples, relative time of measurements, total variation in the reference measurements and so forth. The reason for worse performing PLSR models than Raman spectroscopy might be that NIR spectroscopy exhibits relatively poor sensitivity and selectivity (Blanco & Villarroya, 2002).

3.2.3 Fluorescence spectroscopy

Fluorescence spectroscopy models did not perform particularly well for any of the reference measurements (Table 3). One of the reasons for this might be that samples were excited only at 292 nm, which may not be enough to capture the complexity of intact meat. Another reason for very poor performance regarding drip loss measurements might be that fluorescence spectroscopy is not very sensitive to structural changes responsible for drip development. It has been shown that excitations at longer wavelengths are optimal for fat and connective tissue, at 322 nm and 380 nm, respectively (Skjervold et al., 2003). The reason for choosing the wavelength used in the current experiment was that previous model system experiments have indicated a connection between a shift in the emission spectra from this excitation and changes in pH (Andersen et al., 2017), and it captures the emission from the most fluorescent amino acid, tryptophan, in proteins (Christensen, Norgaard, Bro, & Engelsen, 2006).

4. CONCLUSION

The current study reinforces the perception that Raman spectroscopy is a promising technique for analysis of pork quality. PLSR models for pH and drip loss relied largely on muscle metabolic state and protein structure, while the IMF model relied on characteristic regions for adipose tissue. The information provided in the Raman spectra seems to be appropriate to analyze complex biological systems, like that of meat, and may be applicable for other muscles and species because of the universal nature of post-mortem metabolism. NIR performed poorly in the current study, but has shown good ability to analyze meat quality in earlier studies, and further research is still encouraged. Fluorescence spectroscopy did not show much promise for meat quality assessment, believed in part to be explained by only exciting the samples at one wavelength, thus, fluorescence spectroscopy cannot be ruled out as a possible future technique.

Before addressing the need for development of instruments applicable for testing in abattoir conditions, an effort should be put forth to improve upon the current experiment, by for example, analyzing the same sample with spectroscopy and the reference method and minimizing the delay between spectroscopic analysis and reference analysis. There is also a need to evaluate the optimal time of analysis post-mortem for a given parameter, both for improvement of models and for utilization of the results, which in a large part depends on the workflow in the abattoir. In conclusion, our results encourage further research focusing on the possible applications of Raman spectroscopy to assess meat quality.

Acknowledgements

We thank Bjørg Narum, Karen Wahlstrøm Sanden, Lene Øverby and Vibeke Høst for technical assistance during sampling and with the analyses. Animalia AS is thanked for their generous sharing of data from their analyses. We also thank Prof. Tormod Næs for assistance in experimental design and data analysis, Dr. Kristian Liland for assistance in pre-processing of spectroscopic data and Dr. Nils Kristian Afseth for critical comments on the manuscript. This work was supported by the Foundation for Research Levy on Agricultural products and the Agricultural Agreement Research Fund of Norway.

6. REFERENCES

Andersen, P. V., Veiseth-Kent, E., & Wold, J. P. (2017). Analyzing pH-induced changes in a myofibril model system with vibrational and fluorescence spectroscopy. *Meat Science, 125*, 1-9.

Barnes, R. J., Dhanoa, M. S., & Lister, S. J. (1989). Standard normal variate transformation and de-trending of near-infrared diffuse reflectance spectra. *Applied Spectroscopy, 43*(5), 772-777.

Beattie, J. R., Bell, S. E. J., Borgaard, C., Fearon, A., & Moss, B. W. (2006). Prediction of adipose tissue composition using Raman spectroscopy: Average properties and individual fatty acids. *Lipids, 41*(3), 287-294.

Blanco, M., & Villarroya, I. (2002). NIR spectroscopy: a rapid-response analytical tool. *Trac-Trends in Analytical Chemistry, 21*(4), 240-250.

Brondum, J., Munck, L., Henckel, P., Karlsson, A., Tornberg, E., & Engelsen, S. B. (2000). Prediction of water-holding capacity and composition of porcine meat by comparative spectroscopy. *Meat Science, 55*(2), 177-185.

Christensen, J., Norgaard, L., Bro, R., & Engelsen, S. B. (2006). Multivariate autofluorescence of intact food systems. *Chemical Reviews, 106*(6), 1979-1994.

Christensen, L. B. (2003). Drip loss sampling in porcine M. longissimus dorsi. *Meat Science, 63*(4), 469-477.

Florowski, T., Florowska, A., Chmiel, M., Adamczak, L., Pietrzak, D., & Ruchlicka, M. (2017). The effect of pale, soft and exudative meat on the quality of canned pork in gravy. *Meat Science, 123*, 29-34.

Fowler, S. M., Ponnampalam, E. N., Schmidt, H., Wynn, P., & Hopkins, D. L. (2015). Prediction of intramuscular fat content and major fatty acid groups of lamb M. longissimus lumborum using Raman spectroscopy. *Meat Science, 110*, 70-75.

Gardner, M. A., Huff Lonergan, E., & Lonergan, S. M. (2005). *Prediction of fresh pork quality using indicators of protein degradation and calpain activation*. Paper presented at the 51st International Congress of Meat Science and Technology, Baltimaore, Maryland USA.

Gjerlaug-Enger, E., Aass, L., Odegard, J., & Vangen, O. (2010). Genetic parameters of meat quality traits in two pig breeds measured by rapid methods. *Animal, 4*(11), 1832-1843.

Honikel, K. O. (1998). Reference methods for the assessment of physical characteristics of meat. *Meat Science, 49*(4), 447-457.
Huff-Lonergan, E., & Lonergan, S. M. (2005). Mechanisms of water-holding capacity of meat: The role of postmortem biochemical and structural changes. *Meat Sci, 71*(1), 194-204.
Hughes, J. M., Oiseth, S. K., Purslow, P. P., & Warner, R. D. (2014). A structural approach to understanding the interactions between colour, water-holding capacity and tenderness. *Meat Science, 98*(3), 520-532.
Isaksson, T., Nilsen, B. N., Togersen, G., Hammond, R. P., & Hildrum, K. I. (1996). On-line, proximate analysis of ground beef directly at a meat grinder outlet. *Meat Science, 43*(3-4), 245-253.
Joo, S. T., Kauffman, R. G., Kim, B. C., & Park, G. B. (1999). The relationship of sarcoplasmic and myofibrillar protein solubility to colour and water-holding capacity in porcine longissimus muscle. *Meat Science, 52*(3), 291-297.
Kapper, C., Klont, R. E., Verdonk, J. M. A. J., Williams, P. C., & Urlings, H. A. P. (2012). Prediction of pork quality with near infrared spectroscopy (NIRS) 2. Feasibility and robustness of NIRS measurements under production plant conditions. *Meat Science, 91*(3), 300-305.
Krimm, S., & Bandekar, J. (1986). Vibrational spectroscopy and conformation of peptides, polypeptides, and proteins. *Advances in Protein Chemistry, 38*, 181-364.
Kristensen, L., & Purslow, P. P. (2001). The effect of ageing on the water-holding capacity of pork: role of cytoskeletal proteins. *Meat Science, 58*(1), 17-23.
Lawrie, R. A. (1985). Chapter 10 - The eating quality of meat *Meat Science (Fourth Edition)* (pp. 169-207): Pergamon.
Li-Chan, E. C. Y. (1996). The applications of Raman spectroscopy in food science. *Trends in Food Science & Technology, 7*(11), 361-370.
Li-Chan, E. C. Y., Ismail, A. A., Sedman, J., & van de Voort, F. R. (2002). Vibrational spectroscopy of food and food products *Handbook of Vibrational Spectroscopy*: John Wiley & Sons, Ltd.
Liao, Y. T., Fan, Y. X., & Cheng, F. (2010). On-line prediction of fresh pork quality using visible/near-infrared reflectance spectroscopy. *Meat Science, 86*(4), 901-907.
Lieber, C. A., & Mahadevan-Jansen, A. (2003). Automated method for subtraction of fluorescence from biological Raman spectra. *Applied Spectroscopy, 57*(11), 1363-1367.
Liland, K. H., Kohler, A., & Afseth, N. K. (2016). Model-based pre-processing in Raman spectroscopy of biological samples. *Journal of Raman Spectroscopy, 47*(6), 643-650.
Martens, H., & Martens, M. (2000). Modified Jack-knife estimation of parameter uncertainty in bilinear modelling by partial least squares regression (PLSR). *Food Quality and Preference, 11*(1-2), 5-16.
Martens, H., & Martens, M. (2001). *Introduction to multivariate data analysis for understanding quality*. Chichester, U.K.: John Wiley & Sons Ltd.

Osborne, B. G. (2006). Near-infrared spectroscopy in food analysis *Encyclopedia of Analytical Chemistry*: John Wiley & Sons, Ltd.

Otto, G., Roehe, R., Looft, H., Thoelking, L., & Kalm, E. (2004). Comparison of different methods for determination of drip loss and their relationships to meat quality and carcass characteristics in pigs. *Meat Science, 68*(3), 401-409.

Pedersen, D. K., Morel, S., Andersen, H. J., & Balling Engelsen, S. (2003). Early prediction of water-holding capacity in meat by multivariate vibrational spectroscopy. *Meat Science, 65*(1), 581-592.

Prevolnik, M., Candek-Potokar, M., Skorjanc, D., Velikonja-Bolta, S., Skrlep, M., Znidarsic, T., & Babnik, D. (2005). Predicting intramuscular fat content in pork and beef by near infrared spectroscopy. *Journal of near Infrared Spectroscopy, 13*(2), 77-85.

Prieto, N., Pawluczyk, O., Dugan, M. E. R., & Aalhus, J. L. (2017). A review of the principles and applications of near-infrared spectroscopy to characterize meat, fat, and meat products. *Applied Spectroscopy, 71*(7), 1403-1426.

Prieto, N., Roehe, R., Lavin, P., Batten, G., & Andres, S. (2009). Application of near infrared reflectance spectroscopy to predict meat and meat products quality: A review. *Meat Science, 83*(2), 175-186.

Rasmussen, A. J., & Andersson, M. (1996, 1-6 September). *New method for determination of drip loss in pork muscles.* Paper presented at the In Proceedings 42nd international congress of meat science and technology, Lillehammer, Norway.

Rimai, L., Cole, T., Parsons, J. L., Hickmott, J. T., & Carew, E. B. (1969). Studies of Raman spectra of water solutions of adenosine tri- di- and monophosphate and some related compounds. *Biophysical Journal, 9*(3), 320-&.

Scheier, R., Bauer, A., & Schmidt, H. (2014). Early postmortem prediction of meat quality traits of porcine semimembranosus muscles using a portable Raman system. *Food and Bioprocess Technology, 7*(9), 2732-2741.

Scheier, R., Kohler, J., & Schmidt, H. (2014). Identification of the early postmortem metabolic state of porcine M. semimembranosus using Raman spectroscopy. *Vibrational Spectroscopy, 70*, 12-17.

Scheier, R., Scheeder, M., & Schmidt, H. (2015). Prediction of pork quality at the slaughter line using a portable Raman device. *Meat Science, 103*, 96-103.

Scheier, R., & Schmidt, H. (2013). Measurement of the pH value in pork meat early postmortem by Raman spectroscopy. *Applied Physics B-Lasers and Optics, 111*(2), 289-297.

Schmidt, H., Sowoidnich, K., & Kronfeldt, H. D. (2010). A prototype hand-held raman sensor for the in situ characterization of meat quality. *Applied Spectroscopy, 64*(8), 888-894.

Segtnan, V. H., Sasic, S., Isaksson, T., & Ozaki, Y. (2001). Studies on the structure of water using two-dimensional near-infrared correlation spectroscopy and principal component analysis. *Analytical Chemistry, 73*(13), 3153-3161.

Skjervold, P. O., Taylor, R. G., Wold, J. P., Berge, P., Abouelkaram, S., Culioli, J., & Dufour, E. (2003). Development of intrinsic fluorescent multispectral imagery

specific for fat, connective tissue, and myofibers in meat. *Journal of Food Science, 68*(4), 1161-1168.
Torley, P. J., D'Arcy, B. R., & Trout, G. R. (2000). The effect of ionic strength, polyphosphates type, pH, cooking temperature and preblending on the functional properties of normal and pale, soft, exudative (PSE) pork. *Meat Science, 55*(4), 451-462.
Tu, A. T. (1986). *Spectroscopy of Biological Systems*: Wiley.
Warriss, P. D., & Brown, S. N. (1987). The relationships between initial pH, reflectance and exudation in pig muscle. *Meat Science, 20*(1), 65-74.
Weeranantanaphan, J., Downey, G., Allen, P., & Sun, D. W. (2011). A review of near infrared spectroscopy in muscle food analysis: 2005-2010. *Journal of near Infrared Spectroscopy, 19*(2), 61-104.
Williams, P. (2014). The RPD statistic: A tutorial note. *NIR news, 25*(1), 22-26.
Williams, P., & Norris, K. H. (2001). *Near-infrared technology: In the agricultural and food industries*: American Association of Cereal Chemists.
Williams, P. C., & Sobering, D. C. (1993). Comparison of commercial near infrared transmittance and reflectance instruments for analysis of whole grains and seeds. *Journal of Near Infrared Spectroscopy, 1*(1), 25-32.

Table 1. Mean value, minimum and maximum value, standard deviation (SD) and SD divided by range for reference measurements (n = 122, except for VD where n = 103).

	Mean	Min	Max	SD	SD/range
pH_u	5.46	5.29	5.66	0.08	0.21
EZ-drip %	7.9	3.9	12.4	1.8	0.21
VD %	6.3	3.7	8.8	1.1	0.21
IMF	1.1	0.8	1.6	0.17	0.21

536 **Table 2.** Correlation between quality measurements (n = 122, except for VD where n = 103).
537 (* denotes significant correlation with $p < 0.05$).

	pH_u	EZ-drip %	VD %
EZ-drip %	-0.48*		
VD %	-0.30*	0.60*	
IMF	0.03	-0.30*	-0.22*

538

539

Table 3. Performance of PLSR models from Raman , NIR and fluorescence spectroscopy vs. reference measurements. EZ = EZ-DripLoss in %, VD = vacuum drip loss in % and IMF = intramuscular fat in %.

		n	r_{cv}^2	*RMSECV*	*Factors*	*RPD*
Raman	*EZ*	121	0.49	1.24	3	1.43
	VD	103	0.50	0.75	4	1.41
	pH_u	122	0.52	0.06	3	1.35
	IMF	122	0.73	0.09	5	1.93
NIR	*EZ*	119	0.06[b]	1.69	1	1.05
	VD	101	0.12[b]	1.00	3	1.06
	pH_u	120	0.28[a]	0.07	3	1.16
	IMF	120	0.57[b]	0.11	12	1.58
Fluorescence	*EZ*	121	0.10	1.66	2	1.07
	VD	103	0.04	1.05	1	1.01
	pH_u	122	0.06	0.08	4	1.01
	IMF	122	0.18	0.16	4	1.09

[a] SNV 400-1850 nm

[b] SNV 780-1850 nm

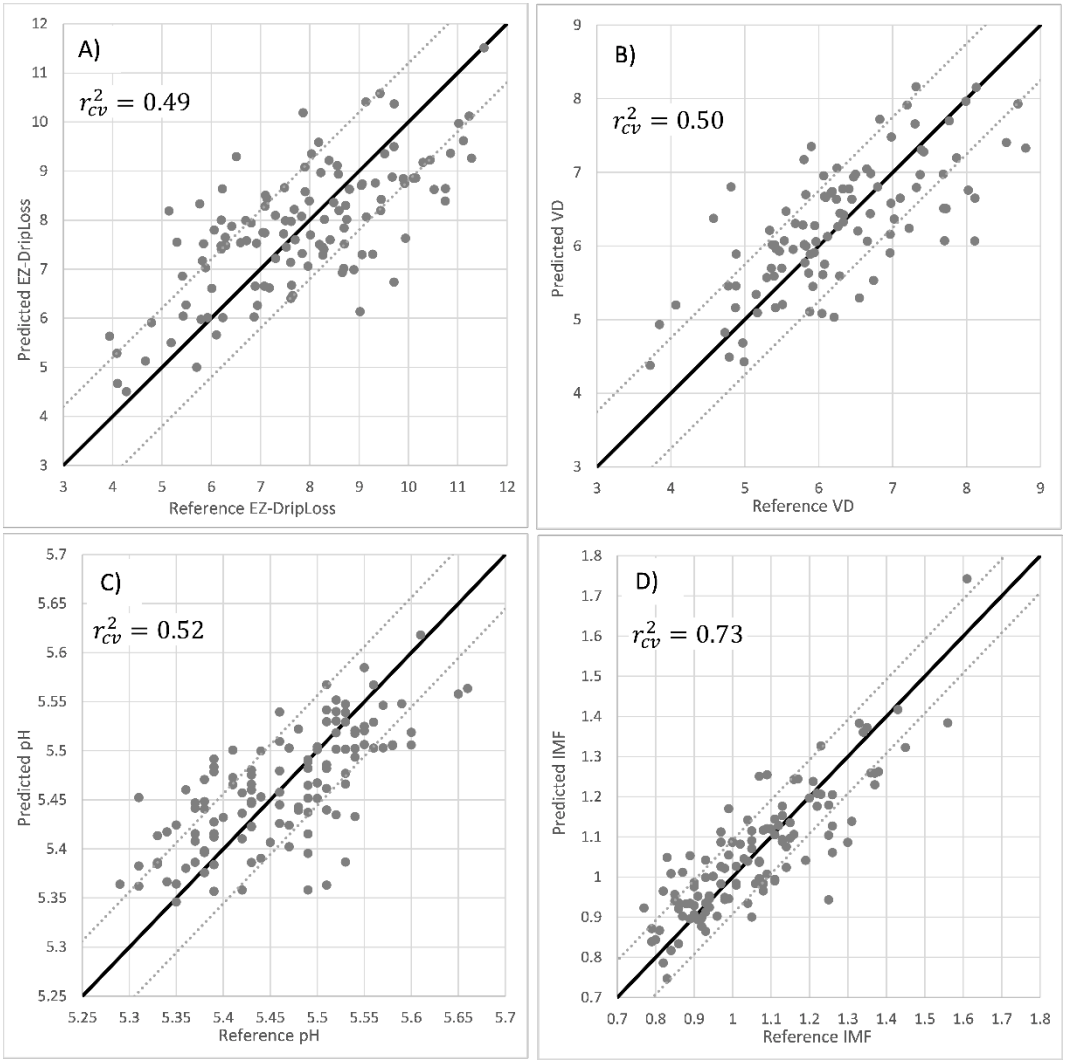

556

557 **Figure 1.** Predicted versus reference measurement plots showing results of PLSR from
558 Raman spectroscopy, where target line is shown as a solid line and RMSECV for each model
559 as dotted lines. A) EZ-DripLoss in %, B) Vacuum drip loss (VD) in %, C) pH and D)
560 intramuscular fat (IMF) in %.

561

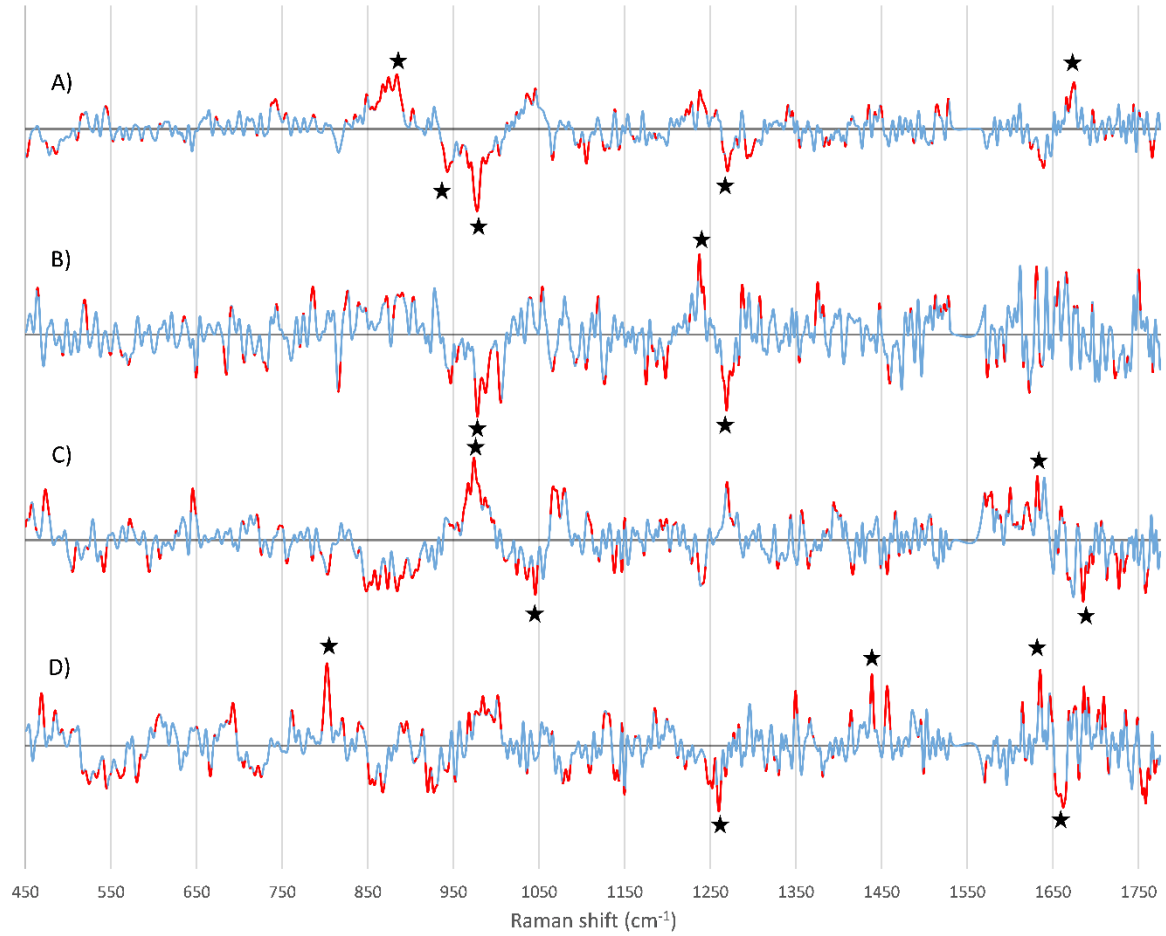

562

563 **Figure 2.** Regression coefficients from PLSR models for A) EZ-DripLoss, B) vacuum drip
564 loss, C) pH and D) intramuscular fat. Regions determined to be significant according to
565 uncertainty test are colored red. Spectral regions referred to in the discussion are marked with
566 stars.

567